Biomedical Materials & Devices (2023) 1:5–20
https://doi.org/10.1007/s44174-022-00040-1

REVIEW

Laser-Induced Forward Transfer on Regenerative Medicine Applications

Christina Kryou[1] · **Ioanna Zergioti**[1,2,3]

Received: 12 July 2022 / Accepted: 12 September 2022 / Published online: 8 December 2022

Abstract

To date, the ultimate goal of bioprinting is to create autologous tissue grafts for future replacement therapies through utilization of cells and biomaterials simultaneously. Bioprinting is an additive manufacturing technology that has significant potential in the biomedical field. Among the main bioprinting techniques, such as inkjet, laser and extrusion bioprinting, the laser-induced forward transfer technique (LIFT) is based on a precise nozzle-free laser-assisted cell free/cell-laden microdroplet transfer. Although this technique was first reported in the 1980s, it begun to rapidly develop in biomedicine only a decade ago. It is a promising technique due to its high spatial resolution, post-bioprinting cell viability, and the ability to deposit high-viscous biomaterials. These characteristics allow the LIFT technology to control cells precisely to engineer living tissue. In this review, we discuss LIFT technique and its applications in biomedical engineering. This advanced technology enables the precise manipulation of in vitro cellular microenvironments and the ability to engineer functional three-dimensional (3D) tissues with high complexity and heterogeneity, which serve in regenerative medicine and in vitro screening applications. The core of this review is the discussion of biological and physical aspects for tissue engineering and/or organ replacement encountered during printing specifically when utilizing the LIFT technique.

Keywords Laser-induced forward transfer · Cell printing · Tissue engineering · LIFT applications · Regenerative medicine

Introduction

The multidisciplinary field of bioprinting combines additive manufacturing process, medical science and mechanical engineering. In recent years, there have been enormous developments in utilizing the potential of bioprinting in different fields including medical sciences [1]. Based on the technology of additive manufacturing method, it can create complex 3D structures by depositing biomaterials on a receiver substrate or scaffold. The advancement of bioprinting ensures its wide prospects in biofabrication, especially in drug testing, tissue engineering, 3D tissue models and regenerative medicine applications [2, 6].

✉ Ioanna Zergioti
zergioti@central.ntua.gr

[1] Department of Physics, National Technical University of Athens, 15780 Zografou, Greece

[2] Institute of Communication and Computer Systems, 15780 Zografou, Greece

[3] PhosPrint P.C., Lefkippos Attica Technology Park, 15341 Agia Paraskevi, Greece

The main objective of bioprinting field is to fabricate functional organs or tissues for in vivo transplantations that can mimic the complexity of native tissues and organs [7, 8]. Native tissues or organs are composed of multiple cell types located within a complex spatially organized three-dimensional microenvironment. In the past, due to limitations in technology, most cells or tissues are cultured in 2D structures. Due to the limited cell interaction in a 2D structure, cells may lose some of their biological functions, causing difficulties in cell migrations, reproduction, and assembly processes for tissue regeneration [9, 11]. In order to overcome these issues, several technologies have been developed to construct 3-D biological models. The latest technologies include bioprinting [12] and microfluidic devices [13]. In recent years, three-dimensional (3D) bioprinting has a potential among all other methods for creating functional tissues to bridge the gap between artificially engineered tissue constructs and native tissues [14, 16].

Bioprinting technologies for engineering functional tissues that mimic their native prototypes fall into four three categories: (i) droplet-based, (ii) extrusion-based, and (iii) laser-based bioprinting techniques. Each of these can be

further classified depending on the specific mechanisms that enable materials or cells to be positioned in 2D or 3D [17, 23–25]. Drop-on demand inkjet bioprinting is the most common technique and used for the printing of matrices for the cell growth (e.g., small scaffolds) [26, 27]. Significant studies of inkjet bioprinting have included the regeneration of functional tissues, such as skin and cartilage, in situ [28, 29]. Nevertheless, inkjet bioprinting has a significant obstacle in material viscosity due to the excessive force required to eject droplets using biomaterials at higher viscosities [30]. Another limitation of this technique is the difficulty in achieving biologically relevant cell densities, thus low cell concentrations are used to facilitate droplet formation (less than 106 cells/mL) [31]. Extrusion-based bioprinting system generates continuous biomaterial filaments enabling sequential layer-by-layer printing and avoiding contamination between different materials, instead of droplets. This technique provides the ability to deposit high cell densities as well biological material such as hydrogels and biocompatible copolymers [32]. Extrusion bioprinting technique has also been used for the generation of multiple tissue types, including aortic valves and in vitro pharmacokinetic models [33, 34]. However, a major drawback of this technique is that cell viability is lower than that with inkjet-based bioprinting (40–86%). The reduced survival rate is probably due to the shear stresses exerted on cells in viscous biomaterials [35]. Although all of these bioprinting technologies find their applications in tissue engineering and regeneration, this review will focus on laser-based technologies and in particular in laser-induced forward transfer technique (LIFT) due to its great potential in bioprinting, and unique technical challenges.

The LIFT technique has been used to create scaffolds, using a wide range of biomaterials, with defined structures [36–38]. LIFT has demonstrated unique properties in bioprinting of various cell-laden/biomaterials for implantable medical devices and tissue engineering/ regenerative medicine applications. As described in the literature, this technique has been applied to print various biomaterials, including proteins [39, DNA [40, living cells [41, 42, and cell-encapsulating hydrogels [43, 44]. Compared to other bioprinting techniques, such as orifice-based inkjet printing, which has some limitations, such as nozzle clogging [45], LIFT, as an orifice-free printing method, has advantages in direct writing cell-laden materials with different viscosities ranging from 1 to 300 mPa/s, with negligible effect on cell viability/cells- functions, and achieves high-resolution printing at cell concentrations up to 1×10^8 cells/mL [46, 47]. Finally, through LIFT printing, the spatial arrangement of cell-laden biomaterials can be controlled at a resolution of less than 10 µm, enabling the fundamental understanding of cell–cell and cell–microenvironment interactions. Although LIFT is one of the most promising bio-printing technique, it has also some limitations in terms of the preparation of the donor supply. The cost of laser-assisted printing technologies is rapidly decreasing due to higher demand as the need for the fabrication of complex bioengineered tissue constructs have increased nowadays. Also, the cost of the process is expected to further decrease as a result of the further decrease of the lasers' cost.

This review will provide a brief overview of the main physical and biological aspects of LIFT bioprinting, as well as present a context that both biologists and physicists can understand.

In the following sections, first the LIFT printing technology is presented from a technical point of view, and the physics behind the technology is described. Then, the physical parameters that must be tuned to print viable cell patterns with respect to cell-level spatial resolution in high-throughput conditions are considered. Finally, tissue engineering and regenerative medicine applications for basic biology research are addressed.

LIFT Bioprinting

Experimental Setup

In principle, the LIFT setup consists of a pulsed laser and two positioning systems namely donor and receiver substrates. The donor substrate is a transparent carrier coated with a thin laser-absorbing layer (also called dynamic release layer, DRL), onto which the material under transfer (e.g., cells, biomaterial, hydrogels) is applied and a receiver substrate which is placed at close proximity and in parallel to the donor surface (Fig. 1) [48, 50].

The laser pulses are focused through the laser-absorbing layer, which is vaporized locally in the focal region of the laser beam. Laser absorption causes a high-pressure bubble to form inside the liquid, which rapidly expands to form a thin, fast jet, followed by the separation of each droplet and subsequent transfer of the droplet to the receiver substrate.

Any desired 2D pattern can be created on the receiver substrate, by moving the laser and/or the two substrates independently, while 3D patterns have also been fabricated in a layer-by-layer manner [51].

A 10- to 100-nm-thick layer of metal (gold [52, titanium [53, silver [54]) is usually used as a laser-absorbing layer material. Alternatively, polymeric materials, such as triazene [55, polyimide [56] and polyethylene naphthalate foil [57], have been reported.

These different laser-absorption materials have been researched for different laser bioprinting experiments. Ablating and vaporizing the absorption material generates debris and, in the case of polymer materials, altered chemical substances. These substances may be gaseous and volatile.

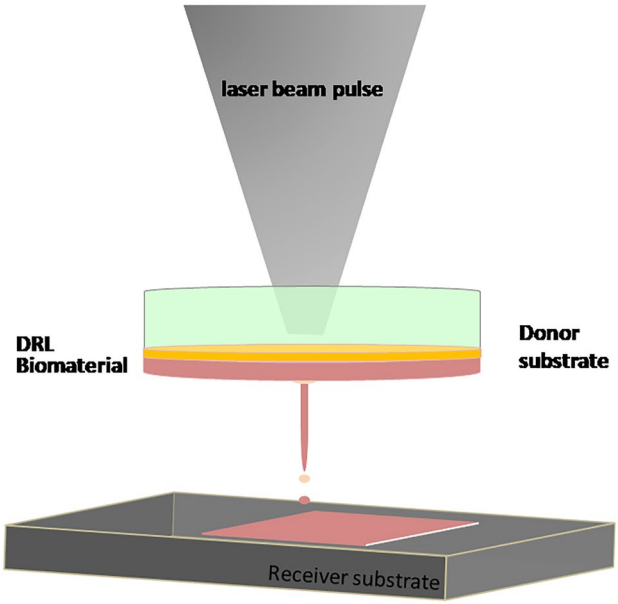

Fig. 1 Schematic of LIFT process

However, some residues are transferred in the printed pattern. However, this is not necessarily a problem, since gold and titanium oxide, for instance, are biologically inert. While these residues may not be readily visible in thicker 3D structures, if one-day complete organs can be printed for implantation, they are likely not to be tolerated. Consequently, the two-layer system of an adhesive cyanoacrylate layer on the glass substrate and a brass foil on top was studied [58]. In this system, the laser pulse only vaporizes cyanoacrylate, causing the vapor bubble to expand and expand the brass foil without disrupting it also known as the "blister effect" [56]. A part of the polyimide directly at the glass slide is evaporated, bulging the remaining part and this blister effect is strong enough to cause biomaterial transfer.

Besides the different laser absorption materials, various laser sources have also been applied. Some research groups applied near-infrared lasers at 1064-nm wavelength [59], while other groups used UV laser sources with wavelengths between 193 [58] and 355 nm [53]. Considering that UV laser sources can induce chemical reactions and break up solid polymers into gaseous substances (in an ideal scenario, this would happen completely), UV lasers are best suited for polymeric absorption materials. However, UV radiation may damage cells.

The use of near-infrared lasers has been limited to metal absorption layers (gold, titanium), resulting in the deposition of debris in the printed structure; however, metal absorption layers are preferred for spreading biomaterials evenly across them.

Parameters Related to LIFT Bioprinting

A number of factors determine the success of LIFT bioprinting, including bubble formation, jet development, deposition volume, resolution, and cell viability. Specifically, the critical parameters include: a) laser fluence, (b)laser spot size, (c) thickness of the laser- absorbing layer, (d) physical properties of the biomaterial, (e) thickness of the biomaterial, (f) distance between donor-receiver substrates [60, 61].

In the jet formation, three regimes appeared by increasing the laser fluence, namely subthreshold regime, jetting regime, and plume regime. These bioprinting regimes are related to the laser-induced bubble dynamic, which can be approximated by the Rayleigh–Plesset equation. This equation, which is the expression of the evolution of the vapor bubble radius with respect to time, depends on the liquid kinematic viscosity of the liquid and the surface tension [62, 63]. The Rayleigh–Plesset equation describes the dynamic of a bubble in an infinite body of incompressible fluid. Since the size of the vapor bubble is not negligible compared to the biomaterial thickness, the interactions of the bubble with the free surface have to be considered. Several studies have demonstrated that when a bubble reaches its maximal diameter, it begins to collapse under external pressure, and a jet may form based on the standoff distance [64, 65]

$$\Gamma = \frac{h}{Rmax} \tag{1}$$

In Eq. 1, h is the distance between the initial vapor bubble centroid and the free surface, which depends on the initial thickness of the biomaterial film and $Rmax$ is the maximum bubble radius, which is related to the laser fluence and the bioink viscosity.

Recent time-resolved imaging studies (Fig. 2) demonstrate the importance of interactions between a bubble and its free surface in the formation of a jet and describe a critical vertex angle that establishes the boundary between subthreshold conditions and jetting conditions [66–68].

A time-dependent graph of the vertex angle for subthreshold and jetting conditions is shown in Fig. 3. Due to plasma formation from ablation of the gold layer (DRL), a large vapor bubble is created at first, resulting in a rapid decrease in the vertex angle [69]. By producing a strong impulse, laser ablation produces pressure enclosed within the bubble, which is greater than atmospheric pressure and surface energy. During the first 5 µsec, the expanding bubble deforms the biomaterial by stretching it in a forward direction. At 5 µsec, the influence of surface tension is apparent from the uniform round tip of protrusion. Since the surface tension and viscoelastic properties of the ribbon

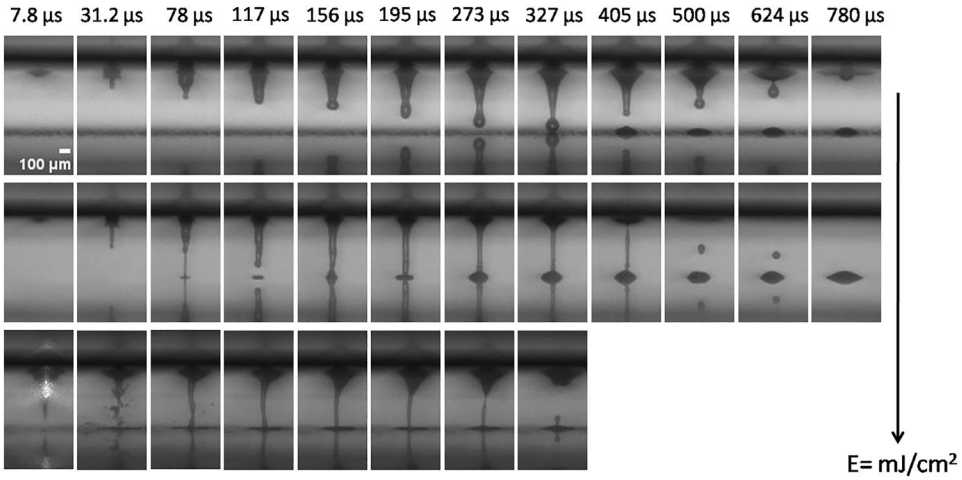

Fig. 2 Time resolved imaging of laser-induced jet formation in LIFT at different laser fluences [66]

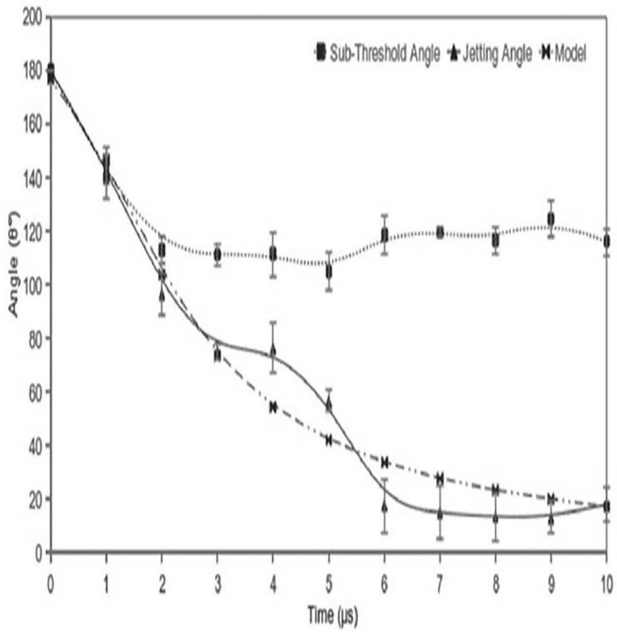

Fig. 3 Vertex angle vs time. Solid curve denotes subthreshold regime, fine dot curve denotes the experimental jetting regime data, and dashed curve denotes the M.S. Longuet-Higgins Model [68]

have counteracted the bubble's expansion, the bubble retreats without generating a jet at 105 degrees. In jetting regime, the vertex angle drops with an abrupt change in behavior at 4 µsec. Initially, the bubble expanded and its vertex angle rapidly decreased, indicating a strong impulse generated by high laser fluence, which accelerated biomaterial forward, allowing it to cross the 105 degrees limits and emerge as a jet at the edge. A rapid deviation from the model at 4 µsec along with the appearance of a spike, demonstrates that biomaterial is involved in maintaining the pressure enclosed inside the liquid. Nevertheless, its viscoelastic properties and external atmospheric pressure cannot overcome the enclosed pressure. During this stage, a spike on the axis may be a result of hydrodynamic pressure concentration at the rear surface of the axis [70]. The continuous propagation is sustained by the momentum [42] of the jet pulling additional fluid from the surrounding film. The counterjet appears as a consequence of momentum conservation. In addition, the protrusion is able to suppress the recoiling process due to surface tension due to fluid induction from the surrounding film in the direction of the flow [71].

In the subthreshold regime, the forming jet returns back to the donor substrate without transferring material. In the plume regime, the breakup of the initial jet and the jet-forming spray resulted in the formation of an unstable jet with undesirable droplets dispersed over the receiver substrate. As a result, both of these regimes are considered undesirable during LIFT bioprinting. During a well-defined bioprinting, a stable jet will appear and the bioink can be transferred in a controlled manner, as demonstrated in Fig. 4b.

At this point, it is important to emphasize that that the laser fluence is not the only parameter that determines the jet regime [72]. The viscosity of biomaterial is also an important parameter here (Fig. 5) [73]. When the biomaterial viscosity is high, it needs more laser fluence to trigger the jet formation process, while if the biomaterial viscosity is low, splashing is very likely to occur. Moreover, during LIFT bioprinting process, printed cells may not survive due to excessive laser fluence transfer or mechanical deformation upon impact on the receiver substrate. In previous studies it has been demonstrated that a minimum shock-absorbing receiving hydrogel substrate (such as MatrigelTM) is necessary for the mechanical shock absorbance of the printed cells. Furthermore, in case the substrate is insufficiently shock-absorbing, sodium alginate can improve cell viability by increasing bio-ink viscosity. Additionally, the laser energy must be adjusted in relation to the maximum radiation dose that the cells can withstand as well as the viscosity of the bio-ink and the shock-absorbing properties of the receiving

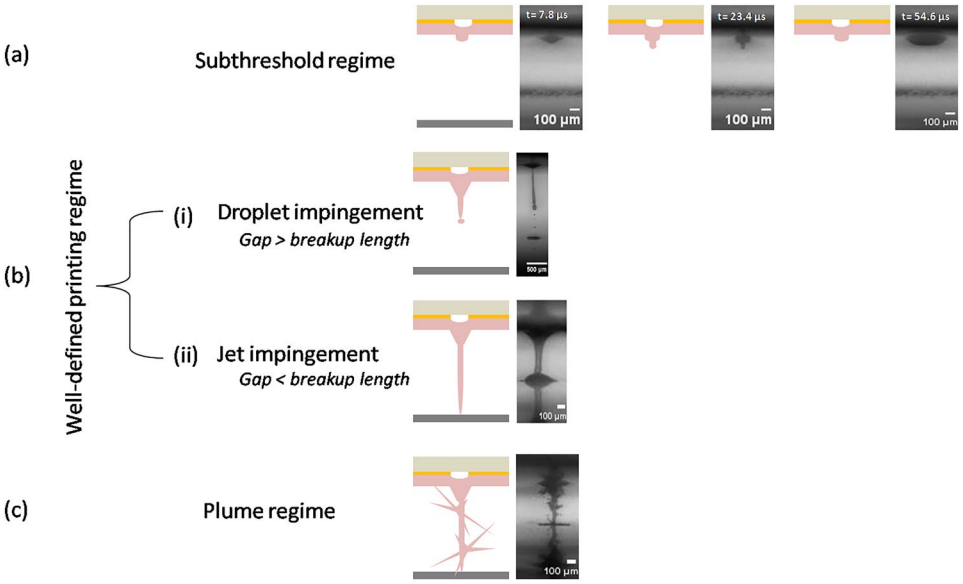

Fig. 4 Schematic of jet formation

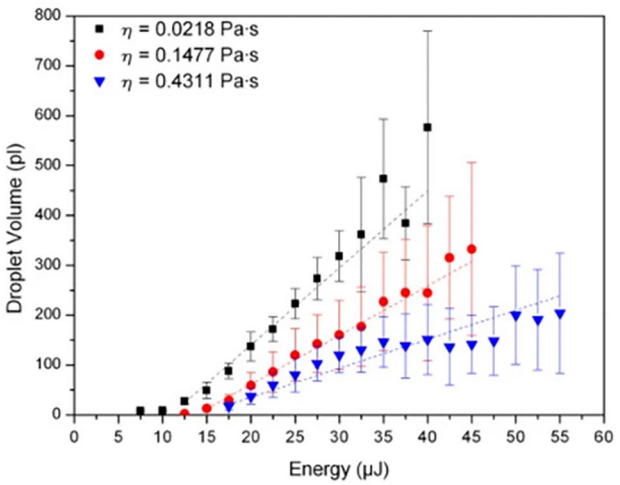

Fig. 5 Influence of layer thickness and viscosity on droplet volume

substrate. So far, no alteration of cell biology caused by LIFT bioprinting (in terms of phenotype and DNA damage) has been reported using suitable parameters.

To our knowledge, the LIFT bioprinting process is valid for engineering cell-containing tissues, but genotoxicity needs to be delineated in cell-based clinical applications before the process can be approved [74, 75].

Controlling the Droplet Volume

The printed droplet volume depends on various parameters. There are some things to consider besides the laser wavelength, pulse duration and laser pulse energy, such as the biomaterial's viscosity, surface tension, the thickness of the laser absorption layer, and the thickness of biomaterial. In terms of viscosity, which is a fundamental material property when studying fluid flow for any application, the most common types of viscosity are dynamic and static, although, in this case, it is the dynamic viscosity that is critical. The relationship between viscosity and shear velocity depends on the material properties. The formation of strong shear forces can destroy cellular structures. Therefore, shear-thinning solution hydrogels, such as collagen, alginate and hyaluronic acid, are beneficial. Typically, a thicker layer results in a larger droplet volume, however viscosity is not systematically influenced by laser pulse energy. Droplet volume increases with increasing viscosity until a maximum value is reached, then it decreases with further increases in hydrogel's viscosity. This effect is even more pronounced with an increased hydrogel layer thickness. Increases in the hydrogel layer thickness increase the specific viscosity at which the printed droplet volume reaches its maximum. During propulsion by the vapor bubble or the hydrogel's jet, their viscosity is decreased, causing a reduction in the shear force on the cells; however, the more shear-thickening hydrogels remain problematic. In general, the volume of a printed droplet ranges from several nanoliters to sub-picoliters, depending on the material used [73].

Effect of LIFT Bioprinting on Cells

Different laser bioprinting setups have been reported to successfully print different types of cells. However, it is possible that the laser-based techniques may introduce thermal and/or mechanical stresses to living cells during laser printing [76, 77]. If these stresses caused by a laser source exceed the ability of cells to adapt, irreversible damage can occur. Thermal and/or mechanical cell injuries as well as biochemical cell injuries are the three main categories of cell damage [78]. Generally, cell damage is reversible up to a certain

point depending on the type and load of damage that a certain cell type can anticipate and/or repair; however, exposure of cells to high external stress may cause irreversible cell injury, even cell death.

Cells do not suffer any damage during the LIFT bioprinting process. This is a critical requirement for implementing bioprinting. For this reason, printed cells need to retain their vitality, behavior, phenotypes, genotypes, and ability to differentiate. Several studies have already been conducted to study cell damage caused by LIFT bioprinting, investigating laser wavelengths ranging from 193 to 1064 nm [79–85] and various pulse durations [86, 87].

For LIFT bioprinting, the most commonly applied laser pulse duration is the nanosecond pulse [39, 88–90]. Nanosecond lasers, however, are capable of causing damage to heat-sensitive cells during bioprinting because of their thermal effects [91]. Short wavelength lasers DNA damage and causes photochemical cross-linking in the cell suspension. As a result, cells can undergo severe genomic instability leading to cell death (apoptosis) or carcinogenesis [92]. It is generally suggested that lasers with shorter pulse duration, such as femtosecond or picosecond lasers, could reduce the heat released to the cell suspension, thus resolving the problem of thermal damage to cells during bioprinting. Among the different types of wavelengths, infrared lasers (IR) are recommended because they cause less damage to cells than UV lasers [46, 93, 94]. However, past studies have revealed that LIFT bioprinting using UV wavelength caused minor damage to the printed cells even without a laser-absorbing layer, in which 99% of the laser energy passes through the cell suspension.

Up to now, several studies have also demonstrated that a variety of mammalian cell types can be laser printed without damaging DNA. Additionally, various other cell types, both carcinoma and normal, exhibit high viability, respectively, of the laser absorbing layer used [95–98]. After bioprinting, cell viability remains between 80 to 90% and even close to 100% (Fig. 6) [22, 99–103]. Moreover, all of these studies show that the cells recover and begin to proliferate normally within a short period of time. Cell viability was determined immediately after LIFT bioprinting. Almost 100% survival rate was described by different groups with different laser sources, laser absorption layers, and cell types.

Barron et al. assessed, through live/dead assay, that 100% of human osteosarcoma cells and MG63 cells retained their viability after LIFT bioprinting [104]. In addition, they measured cell damage after LIFT and showed extremely low expression of stress-induced proteins (i.e., heat- shock proteins) by deposited cells. They demonstrated that LIFT allowed the preservation of cell viability and preserved their ability to establish cell-to-cell communication and to differentiate.

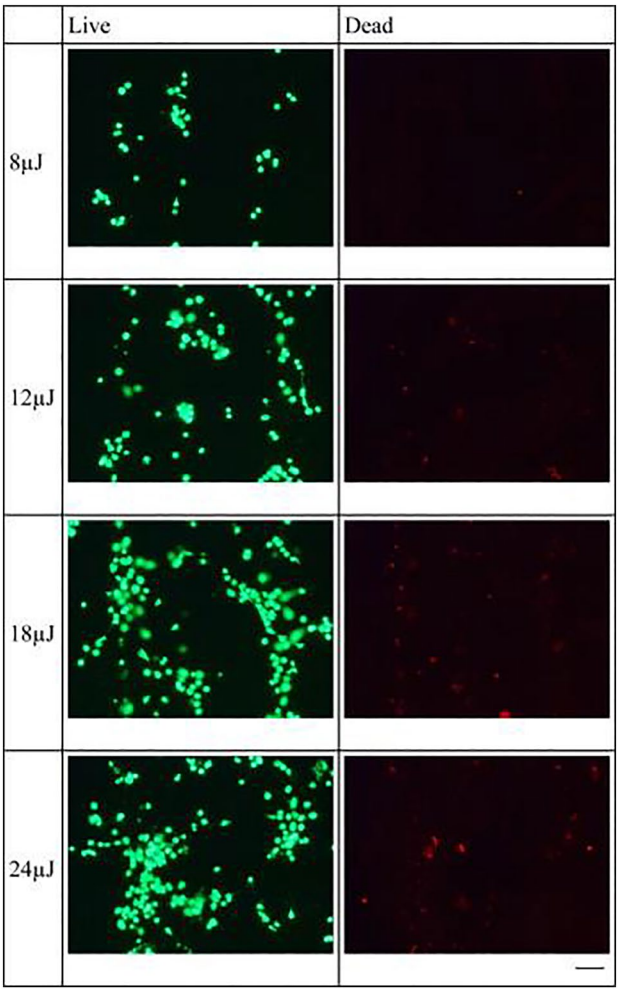

Fig. 6 Effect of laser energy on cell viability. Scale bar = 100 μm [102]

As indicated by the outcomes obtained, several groups made hypotheses and provided explanations related to the influence of the laser process on cell damage. In one of the experiments reported earlier, Ringeisen et al. suggested that the slight cell damage observed after bioprinting was caused by laser incident energy, heat stress, shear stress during acceleration (cell droplets formation) and deceleration (cell droplets landing on receiver substrate) processes. The thickness of hydrogel coating on the receiver slide was found to be an important parameter to decrease cell injury following landing. It was demonstrated that cell viability was increased from 50 to 95% when the hydrogel thickness was raised from 20 to 40 μm [105]. Cell droplets can rupture their membranes during landing, leading to cell death. However, it is possible that cell damage might result from a combination of mechanical, chemical, and photochemical effects [106]. It is possible that the thermal injury affects both enzymes and proteins, potentially causing evaporation or carbonization of cells, and that UV radiation could damage DNA. Lin et al.

determined that laser conditions had a direct effect on cell viability. Based on their experimental results, researchers showed that cell viability of printed yeast (Saccharomyces cerevisiae) decreased with increasing laser energy and that laser energy impacted post-bioprinting cell recovery. However, with regard to thermal and UV damage, they concluded that they were negligible [107].

Interestingly, another study hypothesized that the preservation of cell viability could have been due to the fact that laser-based technologies are high-throughput processes, which subject the cells to rapid stress [108, 109]. As a result, in contrast to the UV damage described earlier by Lin et al., in laser-based technologies used for cell bioprinting, incident laser pulses cause only a small amount of thermal penetration (a few micrometers) compared with 100 µm of thick coating, since jet formation occurs within a few microseconds after incident laser pulses are focused. And, therefore, the thermal damage can be considered negligible [106]. Finally, other groups showed that, in addition to laser energy and hydrogel film thickness, viscosity of cell bioink had a significant effect on maintaining cell viability after bioprinting. The viability of EA.hy926 endothelial cells was determined by applying different laser energies and concentrations of sodium alginate (0.5 or 1% (w/v)), and the results showed that the higher concentration of sodium alginate provided the highest viability. Increasing the bioink viscosity would thus contribute to improve cell survival [110].

In conclusion, laser-based technologies enable the successful bioprinting of a wide variety of cells, while maintaining their viability, genotype, and phenotype [111, 112]. Laser parameters have been optimized in order to protect the cells from the potential damaging effects of the process.

Bioink Composition

In LIFT, cells must be suspended in a liquid bio-ink before being printed onto the receiver substrate, and to print a 3D structure containing cells, the bio-ink should be gelled after bioprinting onto the receiver substrate. Regarding the 3D layer-by-layer manufacturing process, the gelation procedure is necessary to immobilize the 2D- printed structure and to support subsequent bioink layers for 3D structures using the layer-by-layer method, also the gelation procedure should not damage the cells. Especially for LIFT bioprinting applications, bio-inks are demanded to have similar biochemical properties to the native extracellular matrix, which is critical for cell homeostasis in vivo [113, 114]. Several studies have reported that the cells have successfully been printed using different bio-inks including culture medium alone [119, mixed with sodium alginate [116] or a combination of blood plasma and sodium alginate [117].

The human body also contains fibrin gel, which is another example. Gelation starts when fibrinogen is mixed with thrombin. Both hydrogels provide a cell-friendly environment; however, their viscosity is quite low. Therefore, these hydrogels are printed mixed with cells and hyaluronic acid, another hydrogel, which is also found in the human body and has a high viscosity to stiffen the printed structure. Fibrin is also an example of stimulating the migration of keratinocyte cells. It is possible that fibrin-printed cells will reorganize in the printed structure and be found in completely different patterns later [118, 119].

Another hydrogel is collagen, the most abundant structural protein in the human body, however, collagen is acidic, and cells inside would quickly die. Hence, it is necessary to mix it with a base to yield a physiological pH of 7.4 before embedding the cells (after that collagen starts to form a gel). According to the temperature and concentration, the gelation process can take several minutes, although the viscosity changes depending on the level of advanced gelation. As a result of the inhomogeneous viscosity of neutralized collagen with cells, bioprinting with reduced resolution is possible during the gelation process. The gel form of Matrigel or 20% gelatin for bioprinting mouse embryonic stem cells has been successfully created through laser-assisted bioprinting using slightly different techniques [120, 121].

Evaporation of the bioink is critical because it is typically applied into the target as a 50-µm thin layer and therefore, another group has suggested using methyl-cellulose in the bio-ink to prevent evaporation [122].

LIFT-Printed Multicellular Patterns for Cell–Cell and Cell–Microenvironment Interaction Studies

An in-depth understanding of the interactions between different cells and their environments is essential for the development of replacement tissues and organs, as well as cell-based therapies. A conventional cell culture conducted on 2D plastic surfaces is limited in terms of simulating complex interactions within the cell microenvironment, and it cannot simulate 3D tissue microenvironments effectively; cell behavior differs dramatically in three dimensions [123]. In addition to investigating tissue-specific cell behavior, tissue regeneration, and the effects of pharmaceuticals or chemical agents in vivo, printed 3D cell models could provide a better understanding of these topics. For example, complex tissues, especially with integrated vascular networks, have not yet been printed. Even so, the first steps have already been taken. Below follows a presentation of several laser-printed 3D cell constructs, including, a multicellular 3D skin equivalent, stackable biopapers with printed cells, cellularized scaffolds for nerve regeneration and in vivo printing of cardiac patch into mice.

LIFT-Printed Multicellular Patterns for Cell–Cell and Cell–Microenvironment Interaction Studies

Current studies indicate that cell behavior and tissue functionality are influenced by local cell density, cellular spacing, cellular interaction, and binding of cells to their 3D environment, while cellular microarrays have been developed to investigate cell behavior in various experiments in parallel [124, 125]. The ability of LIFT technique to spatially control cell position and to print different cell-laden biomaterials with a various cell-densities may be useful when studying cell–cell and cell–microenvironment interactions [126].

Biological processes are totally different under two-dimensional or three-dimensional culture conditions, so it is necessary to organize cells in three dimensions to reproduce complex intercellular interactions, which occur in vivo [112]. This spatial arrangement of cells has been demonstrated to have important functions on cellular differentiation and cell self-renewal both in vivo and in vitro [127, 129]. A LIFT technique allows researchers to create spatially defined co-cultures or multiculture models through the precise deposit of biomaterials. This allows studying cell communication, identifying cues that drive specific cell differentiation, and investigating how cell–environment interaction affects cell differentiation.

Gruene et al. [130] implemented LIFT for the assembly of multicellular 3D arrays layer-by-layer, consisting of discrete droplets of human adipose-derived stem cells (ASCs) or endothelial colony-forming cells (ECFCs). A 3D array with such a ratio, quantity, type, and spacing can be created with any cellular ratio, quantity, type, or spacing, while the height of the array can be adjusted freely. Fibrinogen and hyaluronic acid formed the natural matrix that acted as a cell carrier. By blade-coating fibrinogen onto a collector slide, first, a layer of fibrin is formed, and then the layer is cross-linked with thrombin. By using LIFT, different cell types are printed in a controlled cell spot spacing on top of the first fibrin layer. Using the same procedure, a second fibrin layer is coated. Finally, the second and third steps can be repeated several times to fabricate 3D cell arrays. Alternatively, the fibrin-based environment can be replaced by any other hydrogel.

ASCs and ECFCs were selected to investigating vascular network formation, since these type of cells represent ideal cell sources for therapeutic revascularization of ischemic tissues and may promote vessel formation in engineered tissue constructs [131].

Cell signaling was observed in vascular endothelial growth factor-free (VEGF-free) medium for 10 days. In addition, 3D mono-coculture cell arrays consisting of ASCs or ECFCs were generated and kept in VEGF-free culture medium as control, and Fig. 7 depicts ASCs (+) that migrated toward the ECFCs (o) and contacted on day 5, while before that the ECFCs showed negligible activity [19]. On day 5, ECFCs activity increased significantly after cell–cell interactions and started to form vascular-like networks, which grew out toward the ASC spots and formed big branches. These vascular-like networks retained their structure stable for 2 weeks under culture conditions and were not observable either in the ASC or the ECFC control. Migration of ASCs toward ECFCs may be driven by a platelet-derived growth factor (PDGF) gradient and the subtype PDGF-BB that is expressed in large amounts by ECFCs is well known to stimulate ASC proliferation and migration [132].

Moreover, using laser-assisted bioprinting of cells to make complex three-dimensional constructs that will replicate native tissues or organs is an application in pharmaceutics and drug development that could replace or at least reduce animal testing [133]. Additionally, this capability to enable studies of cell–cell interactions could be applied to biomaterial (hydrogels) testing and development, by enabling multiple array tests to investigate cell–microenvironment interactions [106].

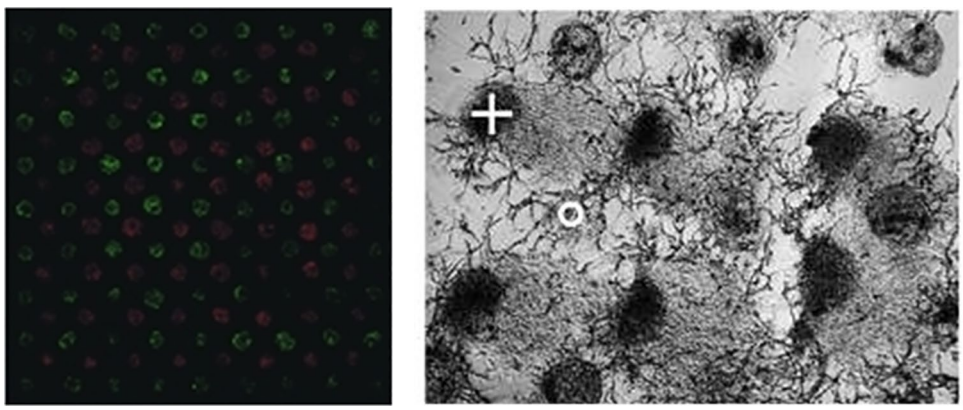

Fig. 7 (left) Fluorescence images demonstrating the variation of cell–cell ratios, (right) visualization of ASCs- ECFCs interactions by 3D cell arrays in co-cultures

Skin Tissue Applications

Ultimately, the objective of bioprinting is to develop 3D organs that fully mimic the native tissue architecture and functions. Although not yet succeeded this goal, simple tissue constructs have already been printed. 3D printed tissue models can be used as testing platforms for chemical agents and pharmaceutical applications. In the future, they could be integrated into so-called micro-physiological systems, which include different ex-vivo tissue types combined in microfluidic systems. Therefore, these printed systems would provide us the ability to understand directly the complex cell's behavior, tissue function, and regeneration.

To investigate the possibility of LIFT tissue formation, researchers developed laser printed skin tissue equivalents as ex vivo tissue models from fibroblast and keratinocyte cell types, both embedded in protein matrices (collagen type I on a collagen-elastin), to mimic the stratified structure of natural skin with a dermis and epidermis [134] (Fig. 8A). These well-established cell types (murine fibroblast, NIH3T3, and human keratinocytes, HaCaT, from adult human skin) were also utilized in past studies [135]. The use of 3T3 fibroblast cells is widespread for keratinocytes culture because they induce favorable growth factors [136]. Collagen which constitutes the main structural element of the dermal extracellular matrix (ECM) in the skin and it was used to reach as close as possible to the native skin.

After LIFT bioprinting, there was evidence that tissue formation was confirmed through the presence of intercellular junctions in all types of tissue, including epithelium like the epidermis.

They investigated intercellular adherens junctions [142, which are essential for tissue morphogenesis, as well as gap junctions, which allow chemical communication between cells [138]. Additionally, researchers also found a significant number of intercellular adherens junction formation between printed keratinocytes and minor formation between fibroblasts, as expected since keratinocytes form a high level of junctions in the dermal epithelium (epidermis) [137] (Fig. 8E). Moreover, a few days after LIFT, they noticed gap junctions, localized within the cell membrane, between all neighboring cells, and using a dye-transfer method in vital 3D cell constructs, the functionality of cell–cell communication was demonstrated. Therefore, printed skin grafts were shown to mimic tissue-specific functions with respect to adherens and gap junctions and basement membrane formation between keratinocytes and fibroblasts, as it appears between the epidermis and dermis in native skin, was also noticed [134] (Fig. 8C).

Michael et al. [139] printed a fully cellularized auxiliary skin using the LIFT technique. These skin substitutes were further tested in vivo using the dorsal skin fold chamber in animal models. These skin substitutes were completely integrated into the neighboring tissue when implanted after

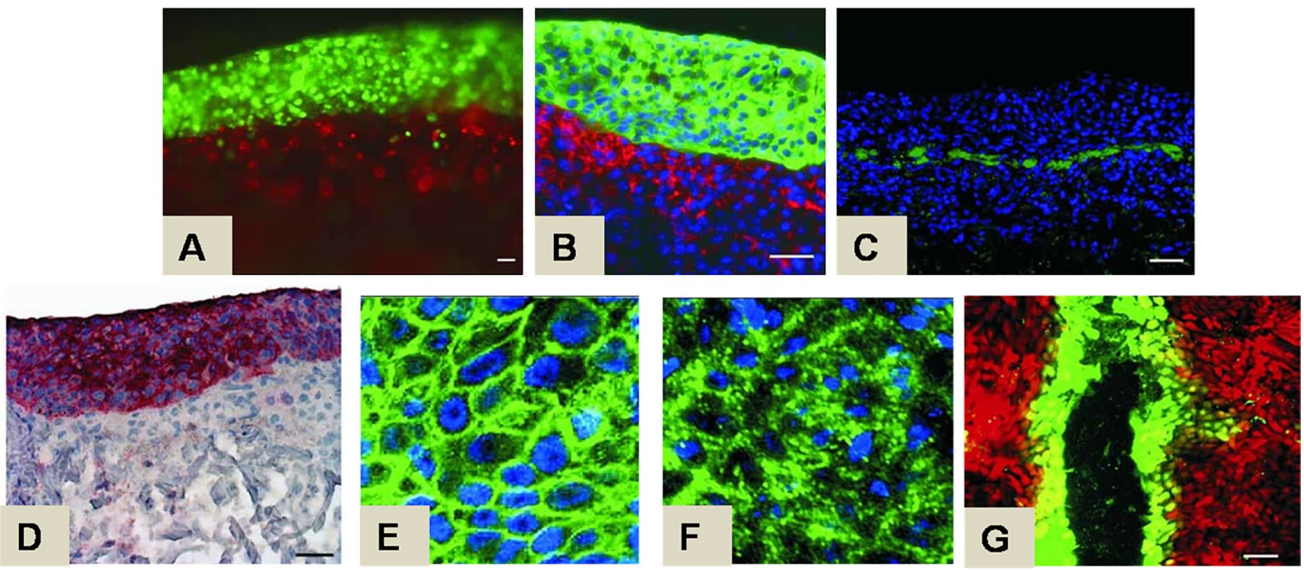

Fig. 8 Skin tissue formation, 10 days after printing. Fluorescence microscopic images of 3D printed fibroblasts and keratinocytes. A) Section through the laser printed structure, prepared directly after LIFT, with transduced fibroblasts (red) and keratinocytes (green),B) fibroblasts are stained in red (pan-reticular fibroblast), keratinocytes are stained in green (cytokeratin 14) and cell nuclei are stained in blue, C) An anti-laminin staining in green and all cell nuclei in blue, D) keratinocytes in the bi-layered structure while all cell nuclei (fibroblasts and keratinocytes) are counterstained in light blue with hematoxylin, E) pan-cadherin-staining (green) and cell nuclei staining with Hoechst (33,342 (blue), F) Cx43 distributed in a scattered, punctate fashion, which is a sign for the formation of gap junctions; G) Visualization of gap junction coupling with Lucifer yellow dye (green), the nuclei of the HaCaT keratinocytes are stained red

11 days and a stratified epidermis with beginning differentiation and stratum corneum was observed. The presence of E-cadherin as a marker for adherens junctions and consequently the formation of tissue could be observed in the epidermis both in vivo and in vitro. LIFT-printed fibroblasts developed collagen above and within the substratal Matriderm in both conditions and the blood vessels appeared to grow from the base of the wound and its edges toward the printed cells.

Blood Vessel Applications

A major challenge of tissue engineering is to create perfusable tissue substitutes, considering that cells are confined to a diffusion distance of 150–200 µm from blood vessels. In numerous studies, different strategies have been used to develop a functional vasculature, e.g., growth factors, pericytes and smooth muscle cells, coculture with different types of cells, and gene transfer. Several LIFT-based studies have targeted this challenging task by using cell bioprinting and prevascularization methods to achieve tissue perfusion via engineered tissues.

Using laser-based technology, researchers patterned HUVECs on MatrigelTM in two and three dimensions and found that vascular structures are formed in accordance with the pattern [140]. Another group demonstrated the capacity of the LIFT technique to organize HUVECs and HUVSMCs in branch/stem structures in order to promote a network organization, similar to an in vivo vasculature [141]. In addition, Pirlo et al. used LIFT bioprinting to print HUVECs on PLGA/hydrogel (Collagen type I from rat tail or Matrigel™) biopapers. They demonstrated that cells self-assembled into networks, following the defined pattern, mimicking the complex vascularization of native tissue. Through overlaying the HUVEC networks on biopaper layers, 3D prevascularized constructs are possible, allowing them to be fabricated in three dimensions [142] (Fig. 9). Using the LIFT technique, microvascular networks have been formed in an oriented and controlled manner, and with the combination of layers-by-layers, it will be possible to enable complete 3D constructions.

It appears that laser-assisted cell bioprinting holds promise as a method to introduce prevascularization within engineered constructs; however, a greater degree of development is needed in order to create fully-functional tissue constructs that can be perfused. Before implantation of three-dimensional substitutes, it is essential to create an environment that promotes the growth of vascular networks and the morphology and function of endothelial cells. Particularly, this recapitulation of a cell-friendly microenvironment is crucial because it enables cell signaling between neighboring cells. As an example, the cardiomyocyte function, including myocardial contractility, is regulated by the coupling of endothelial cells with cardiomyocytes in cardiac surgery [143].

Nervous System Applications

As nervous tissue presents limited healing capacity, tissue engineering faces the challenge of preventing irreversible loss of function when the central and peripheral nervous systems are damaged;. In order to promote nerve repair and regeneration, laser-based technologies have been applied to pattern neurons or glial cells along with a specific architecture within a structure in three dimensions. Researchers printed B35 neuronal cells to create three-dimensional cellularized models, by in situ depth-controlled transfer within polymerized MatrigelTM substrate, to study nerve regeneration [144] (Fig. 10).

A research group used the LIFT technique to print relevant-size patterns of olfactory ensheathing cells (OECs) throughout a multilayer hydrogel scaffold. These cells have shown the ability to promote neurite outgrowth in spinal cord injury models [145]. The authors demonstrated the

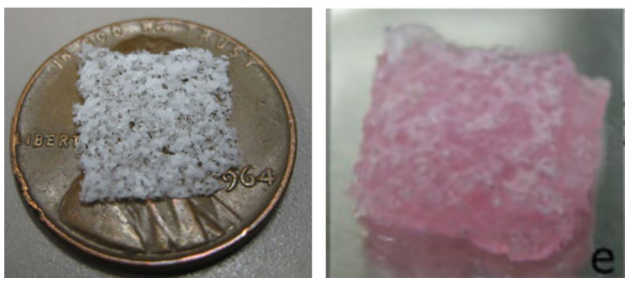

Fig. 9 (left) Unloaded PLGA, (right) Biopaper loaded with HUVECs and Collagen Type I [142]

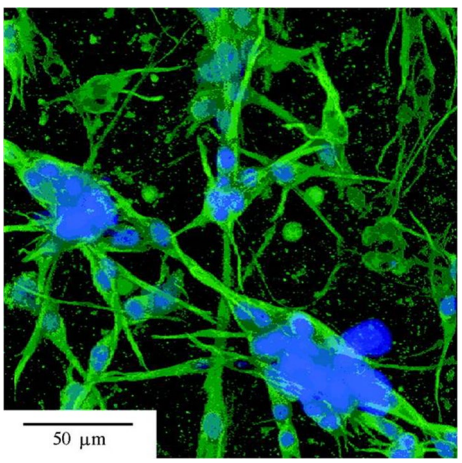

Fig. 10 Observation of printed B35 neuronal cells in confocal microscopy, with the presence of axonal extensions between neuronal cells on different deposition planes [144]

creation of a three-dimensional cellularized scaffold, with a defined micro-organization of OECs, that enhanced cell interactions and proved that these cellularized matrices could be transplantable into an animal model to promote axonal regeneration of spinal cord injury [146].

Additionally, neural stem studies, such as cell proliferation and differentiation, could be performed using laser bioprinting technologies, by organizing the cells along with a specific architecture within a structure, leading to advances in nerve damage treatment or drug testing applications [147]. Moreover, Curley et al. organized the dorsal root ganglion neurons using laser direct write technique in order to reproduce a neural micro physiological system, offering deeper understanding and prospects in neurophysiology and neuro-regeneration [148]. As a result of the inherent complexity of the nervous system, bioprinting techniques such as LIFT can create cellular models that are unsurpassed in terms of cellular organization, thereby expanding the field of regenerative medicine.

Heart Applications

The use of laser bioprinting to create cellular structures holds great promise for the creation of cardiac tissue, as cardiomyocytes are contractile cells with a specific three-dimensional arrangement. The current lack of neovascularization, concerning therapeutic solutions after myocardial infarction, such as cardiac patches, is one of the main limitations. Recent studies have indicated that lasers could be used in bioprinting, leading to significant implications for cardiac surgery.

In order to promote cardiac regeneration, Gaebel et al. printed squared patterns of HUVEC and hMSC onto a polyester urethane urea (PEEUU) patch. The rationale for using hMSC was based on their capacity to stimulate angiogenesis. In fact, the authors found that the formation of coculture patches of HUVEC and hMSCs led to vascularization and improved functional recovery of infarcted hearts when compared to cells seeded randomly. In this way, cell bioprinting could be an effective method for treating myocardial infarction, resulting in wound healing and enhanced cardiac function preservation [149] (Fig. 11).

Several studies have been focused on establishing co-cultures between MSCs and cardiomyocytes since they have been shown to contribute to cardiac regeneration. However, these conventional coculture systems do not accurately mimic native cardiac muscle architecture. Ma et al. present an improved MSC–cardiomyocyte coculture model by using laser-based technologies, which mimic the arrangement of cardiomyocytes in vivo. The aim of the study was to examine whether this cellular cross-talk had an impact on MSC cardiogenic differentiation. According to the results, this cell alignment accelerated stem cell differentiation into the cardiac phenotype (contractile cytoskeleton, electrophysiological properties, cardiogenic transcription factors, and connexin 43 distribution) [150].

In this field of medical research, in addition to its benefits for cardiac repair, LIFT may allow the development of more sophisticated in vitro models, to further understand the cell–cell and cell- environment cardiovascular mechanisms leading to cardiac disorders such as arrhythmia, contractility issues, hypoxia resistance, and sensibility by accurately reproducing the cardiac tissues in three dimensions.

Bone Applications

Today, bone tissue regeneration has proven to be a major public health problem, and many diseases that cause bone loss affects an increasing number of patients due to the aging of the population [151]. Although there is a wide range of therapeutic approaches, all have limitations, such as pain, infections, and morbidity. The major impediment is the insufficient perfusion of bone grafts or bone substitutes, which leads to graft failure [152, 153]. This is an explanation of why bone repair, especially in cases of critical size defects, is still a crucial challenge. There have been multiple approaches proposed for enhancing the microvascularization of tissue-engineered constructs [154].

It's possible to use synthetic or natural biomaterial scaffolds to promote bone injury healing, but these scaffolds lack the osteogenic, osteoinductive properties that can be achieved through bone autografts [155]. From this perspective, several studies have investigated this problem, specifically on the improvement of vascularity and several biological functions, using LIFT bioprinting, with the aim of promoting bone regeneration [156].

Using the LIFT technique, Catros et al. printed human osteoprogenitors (derived from human bone marrow stoma cells) to create two- and three-dimensional composite structures, thus demonstrating that LIFT preserves nHA functionality and cell proliferation and differentiation properties post-bioprinting [157]. The same group did demonstrate the feasibility of adapting the laser workstation for in vivo bioprinting, by transferring nHA particles directly onto a mouse bone calvarias defect [163, however bone repair was not stable, probably due to displacement of the printed material after surgery. Gruene et al. demonstrated that MSC differentiation into osteogenic and chondrogenic lineages was preserved when embedding them in a thin matrix biomaterial (plasma and alginate). They then developed three-dimensional constructs that produced autologous bone and cartilage tissue grafts after being cultured for 2 weeks, enabling their transplantation into animals [81].

In conclusion, LIFT bioprinting could have potential applications in orthopedic and dental tissue engineering, allowing the bone structure to be reproduced with the highest

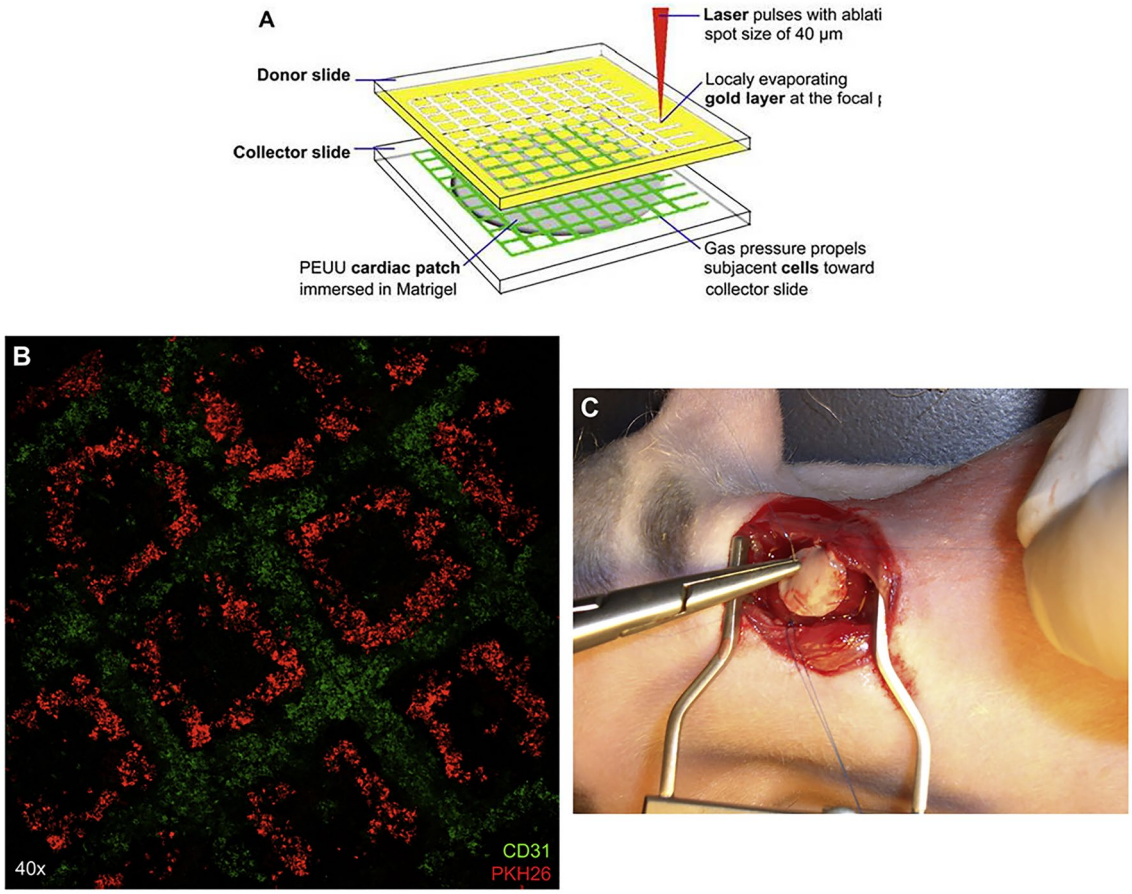

Fig. 11 **a** Schematic representation of laser bioprinting setup. **B**Observation of printed patterns of human MSC and HUVEC on cardiac patches 24 h after bioprinting. **c**Patch implantation in vivo in a rat infarction model [149]

possible accuracy. It is imperative to better understand the cooperation between vascular, osteoblastic, osteoclastic, and neural cells at a cellular level, while at a tissue level; bone organization differs from periphery to center. Ossification differs between endochondral and membranous bones, and reproducing an embryonic environment is critical for optimal bone healing. This technology has the potential to lead to the development of personalized bone models based on ossification and healing types. Additional cell types, such as nerve cells, can also be added to the model to produce more elaborate models.

Conclusion

The review encompasses the concept of LIFT bioprinting, the technical specifications of this technique, and its wide range of applications in research areas. LIFT bioprinting is currently in its early stages of development and has produced a number of impressive results. This versatile technique can accurately reproduce in vitro the microenvironment of cells and the micro-architecture of native tissues, making it an exciting tool for fundamental research, tissue engineering, and regenerative medicine applications. In forthcoming years, advances in technology (robotics, automation, biological and material discoveries) could allow for the transition of LIFT technology from the bench to the bedside.

Author Contributions All authors have read and agreed to the published version of the manuscript.

Funding Open access funding provided by HEAL-Link Greece. The authors acknowledge funding from the EU Horizon 2020 FET program UroPrint under Grant Agreement No 964883.

Data Availability Data is contained within this article.

Declarations

Conflict of interest The authors declare no conflicts of interest.

References

1. C. Mandrycky, Z. Wang, K. Kim, D.H. Kim, Biotechnol. Adv. **34**(4), 422–434 (2016)
2. S.V. Murphy, A. Atala, Nat. Biotechnol. **32**(8), 773–785 (2014)
3. A. Eltom, G. Zhong, A. Muhammad, Scaffold techniques and designs in tissue engineering functions and purposes: a review. Adv. Mater. Sci. Eng. **2019**, 3429527 (2019)
4. R.G. Pearson, R. Bhandari, R.A. Quirk, K.M. Shakesheff, Recent advances in tissue engineering. J. Long-Term Eff. Med. Implants **27**, 199–232 (2017)
5. X. Zhang, Y. Zhang, Tissue engineering applications of three-dimensional bioprinting. Cell Biochem. Biophys. **72**, 777–782 (2015)
6. D.X.B. Chen, Scaffold Design, in *Extrusion bioprinting scaffolds tissue engineering application* (Springer, Dodrecht, 2019), pp.15–30
7. S.V. Murphy, A. Skardal, A. Atala, J. Biomed, Mater. Res. A **101**(1), 272–284 (2013)
8. I.T. Ozbolat, Y. Yu, IEEE Trans. Biomed. Eng. **60**(3), 691–699 (2013)
9. K.L. Schmeichel, M.J. Bissell, J. Cell Sci. **116**(12), 2377–2388 (2003)
10. S. Breslin, L. O'Driscoll, Drug Discov. Today **18**(5–6), 240–249 (2013)
11. J.B. Kim, Semin. Cancer Biol. **15**(5), 365–377 (2005)
12. S.M. Peltola, F.P. Melchels, D.W. Grijpma, M. Kellomaki, Ann. Med. **40**(4), 268–280 (2008)
13. P.J. Lee, N. Ghorashian, T.A. Gaige, P.J. Hung, JALA **12**(6), 363–367 (2007)
14. J.M. Unagolla, A.C. Jayasuriya, Hydrogel-based 3D bioprinting: a comprehensive review on cell-laden hydrogels, bioink formulations, and future perspectives. Appl. Mater. Today **18**, 100479 (2020)
15. M. Moradi, M.K. Moghadam, M. Shamsborhan, M. Bodaghi, H. Falavandi, Post-processing of FDM 3d printed polylactic acid parts by laser beam cutting. Polymers **12**, 550 (2020)
16. Y.S. Zhang, K. Yue, J. Aleman, K. MollazadehMoghaddam, S.M. Bakht, J. Yang, W. Jia, V. Dell'Erba, P. Assawes, S.R. Shin, M.R. Dokmeci, R. Oklu, A. Khademhosseini, 3D bioprinting for tissue and organ fabrication. Ann. Biomed. Eng. **45**, 148–163 (2017)
17. P. Fisch, M. Holub and M. Zenobi-Wong, Improved accuracy and precision of bioprinting through progressive cavity pump-controlled extrusion, 2020, BioRxiv, 2020.01.23.915868.
18. I.T. Ozbolat, M. Hospodiuk, Current advances and future perspectives in extrusion-based bioprinting. Biomaterials **76**, 321–343 (2016)
19. S. Papazoglou, D. Kaltsas, A. Logotheti, A. Pesquera, A. Zurutuza, L. Tsetseris, I. Zergioti, A direct transfer solution for digital laser bioprinting of CVD graphene. 2D Mater. **8**(4), 045017 (2021)
20. Z. Kanaki, C. Chandrinou, I. Orfanou, C. Kryou, J. Ziesmer, G.A. Sotiriou, A. Klinakis, C. Tamvakopoulos, I. Zergioti, Laser-induced forward transfer bioprinting on microneedles for transdermal delivery of gemcitabine. Int. J. Bioprint. **8**, 2 (2022)
21. J.A. Barron, P. Wu, H.D. Ladouceur, B.R. Ringeisen, Biomed. Microdev. **6**(2), 139–147 (2004)
22. J.A. Barron, B.J. Spargo, B.R. Ringeisen, Appl. Phys. A **79**(4–6), 1027–1030 (2004)
23. J.M. Fernandez-Pradas, M. Colina, P. Serra, J. Domınguez, J.L. Morenza, Thin Solid Films **453–454**, 27–30 (2004)
24. R. Kumar, E. Joanni, R. Savu, M.S. Pereira, R.K. Singh, C.J.L. Constantino, L.T. Kubota, A. Matsuda, Energy **179**, 676–684 (2019)
25. E. Joanni, R. Kumar, W.P. Fernandes, R. Savu, A. Matsuda, In situ growth of laser-induced graphene micro-patterns on arbitrary substrates. Nanoscale **14**, 8914–8918 (2022)
26. H. Gudapati, M. Dey, I. Ozbolat, A comprehensive review on droplet-based bioprinting: past, present and future. Biomaterials **102**, 20–42 (2016)
27. C.J. Hansen, R. Saksena, D.B. Kolesky, J.J. Vericella, S.J. Kranz, G.P. Muldowney, K.T. Christensen, J.A. Lewis, High-throughput printing via microvascular multinozzle arrays. Adv. Mater. **25**, 96–102 (2013)
28. A. Skardal, D. Mack, E. Kapetanovic, A. Atala, J.D. Jackson, J. Yoo, S. Soker, Bioprinted amniotic fluid-derived stem cells accelerate healing of large skin wounds. Stem Cells Transl. Med. **1**, 792–802 (2012)
29. X. Cui, K. Breitenkamp, M. Finn, M. Lotz, D.D. D'Lima, Direct human cartilage repair using three-dimensional bioprinting technology. Tissue Eng. Part A. **18**, 1304–1312 (2012)
30. T. Xu, J. Jin, C. Gregory, J.J. Hickman, T. Boland, Inkjet printing of viable mammalian cells. Biomaterials **26**, 93–99 (2005)
31. J.D. Kim, J.S. Choi, B.S. Kim, Y.C. Choi, Y.W. Cho, Piezoelectric inkjet printing of polymers: stem cell patterning on polymer substrates. Polymer **51**, 2147–2154 (2010)
32. V. Mironov, V. Kasyanov, R.R. Markwald, Organ printing: from bioprinter to organ biofabrication line. Curr. Opin. Biotechnol. **22**, 667–673 (2011)
33. B. Duan, L.A. Hockaday, K.H. Kang, J.T. Butcher, 3D bioprinting of heterogeneous aortic valve conduits with alginate/gelatin hydrogels. J. Biomed. Mater. Res. A. **101**, 1255–1264 (2013)
34. R. Chang, J. Nam, W. Sun, Direct cell writing of 3D microorgan for in vitro pharmacokinetic model. Tissue Eng. Part C Methods. **14**, 157–166 (2008). https://doi.org/10.1089/ten.tec.2007.0392
35. R. Chang, J. Nam, W. Sun, Effects of dispensing pressure and nozzle diameter on cell survival from solid freeform fabrication-based direct cell writing. Tissue Eng. Part A. **14**, 41–48 (2008)
36. A. Selimis, V. Mironov, M. Farsari, Direct laser writing: Principles and materials for scaffold 3D printing. Microelectron. Eng. **132**, 83–89 (2015)
37. B. Guillotin, M. Ali, A. Ducom, S. Catros, V. Keriquel, A. Souquet, M. Remy, J.C. Fricain, F. Guillemot, Laser-assisted bioprinting for tissue engineering, in *Biofabrication: Micro- and Nano-Fabrication, Printing, Patterning, and Assemblies*. ed. by G. Forgacs, W. Sun (William Andrew Publishing, Boston, 2013), pp.95–118
38. B.C. Riggs, A.D. Dias, N.R. Schiele, R. Cristescu, Y. Huang, D.T. Corr, D.B. Chrisey, Matrix-assisted pulsed laser methods for biofabrication. MRS Bull. **36**(12), 1043–1050 (2011)
39. V. Dinca, M. Farsari, D. Kafetzopoulos, A. Popescu, M. Dinescu, C. Fotakis, Patterning parameters for biomolecules microarrays constructed with nanosecond and femtosecond UV lasers. Thin Solid Films **516**, 6504–6511 (2008)
40. I. Zergioti, D.G. Papazoglou, A. Karaiskou, C. Fotakis, E. Kapsetaki, D. Kafetzopoulos, Femtosecond Laser Microprinting of Biomaterials. Appl. Phys. Lett. **86**, 163902 (2005)
41. Z. Zhang, C. Xu, R. Xiong, D.B. Chrisey, Y. Huang, Effects of living cells on the bioink printability during laser printing. Biomicrofluidics **11**, 034120 (2017)

42. P.K. Wu, B.R. Ringeisen, Development of Human Umbilical Vein Endothelial Cell (HUVEC) and Human Umbilical Vein Smooth Muscle Cell (HUVSMC) Branch/Stem Structures on Hydrogel Layers Via Biological Laser Printing (BioLP). Biofabrication **2**, 014111 (2010)
43. T.B. Phamduy, N.A. Raof, N.R. Schiele, Z. Yan, D.T. Corr, Y. Huang, Y. Xie, D.B. Chrisey, Laser direct-write of single microbeads into spatially-ordered patterns. Biofabrication **4**, 025006 (2012)
44. L. Ouyang, R. Yao, X. Chen, J. Na, W. Sun, 3D printing of HEK 293FT cell-Laden hydrogel into macroporous constructs with high cell viability and normal biological functions. Biofabrication **7**, 015010 (2015)
45. K. Christensen, C. Xu, W. Chai, Z. Zhang, J. Fu, Y. Huang, Freeform inkjet printing of cellular structures with bifurcations. Biotechnol. Bioeng. **112**, 1047–1055 (2015)
46. F. Guillemot, A. Souquet, S. Catros, B. Guillotin, J. Lopez, M. Faucon, B. Pippenger, R. Bareille, M. Remy, S. Bellance, P. Chabassier, J.C. Fricain, J. Amedee, Acta Biomater. **6**(7), 2494–2500 (2010)
47. V.S. Cheptsov, S.I. Tsypina, N.V. Minaev, V.I. Yusupov, B. Chichkov, Int. J. Bioprint. **5**(1), 165 (2018)
48. L. Moroni, T. Boland, J.A. Burdick, C. De Maria, B. Derby, G. Forgacs, J. Groll, Q. Li, J. Malda, V.A. Mironov, C. Mota, Biofabrication: a guide to technology and terminology. Trends Biotechnol **36**(4), 384–402 (2018)
49. M. Hospodiuk, M. Dey, D. Sosnoski, I.T. Ozbolat, The bioink: a comprehensive review on bioprintable materials. Biotechnol Adv. **35**(2), 217–239 (2017)
50. D. Nguyen, D.A. Hägg, A. Forsman, J. Ekholm, P. Nimkingratana, C. Brantsing, T. Kalogeropoulos, S. Zaunz, S. Concaro, M. Brittberg, A. Lindahl, Cartilage tissue engineering by the 3D bioprinting of iPS cells in a nanocellulose/alginate bioink. Sci. Rep. **7**(1), 1–10 (2017)
51. S.F. Badylak, T.W. Gilbert, Immune response to biologic scaffold materials, in *Seminars in immunology*, vol. 20, (Academic Press, San Diego, CA, 2008), pp.109–116
52. V. Dinca, A. Ranella, A. Popescu, M. Dinescu, M. Farsari, C. Fotakis, Parameters optimization for biological molecules patterning using 248-nm ultrafast lasers. Appl. Surf. Sci. **254**, 1164–1168 (2007)
53. M. Duocastella, J.M. Fernandez-Pradas, J.L. Morenza, P. Serra, Sessile droplet formation in the laser-induced forward transfer of liquids: a time-resolved imaging study. Thin Solid Films **518**, 5321–5325 (2010)
54. B. Hopp, T. Smausz, N. Kresz, N. Barna, Z. Bor, L. Kolozsvari, D.B. Chrisey, A. Szabo, A. Nogradi, Survival and proliferative ability of various living cell types after laser-induced forward transfer. Tissue Eng. **11**(11–12), 1817–1823 (2005)
55. A. Palla-Papavlu, I. Paraico, J. Shaw-Stewart, V. Dinca, T. Savopol, E. Kovacs, T. Lippert, A. Wokaun, M. Dinescu, Liposome micropatterning based on laser-induced forward transfer. Appl. Phys. A **102**(3), 651–659 (2011)
56. M.S. Brown, C.F. Brasz, Y. Ventikos, C.B. Arnold, Impulsively actuated jets from thin liquid films for high resolution bioprinting applications. J. Fluid Mech. **709**, 341–370 (2012)
57. A. Vogel, K. Lorenz, V. Horneffer, Mechanisms of laser-induced dissection and transport of histologic specimens. Biophys. J. **93**, 4481–4500 (2007)
58. Y. Lin, Y. Huang, D.B. Chrisey, Metallic foil-assisted laser cell bioprinting. J. Biomech. Eng. **133**, 025001 (2011)
59. S. Catros, F. Guillemot, A. Nandakumar, S. Ziane, L. Moroni, P. Habibovic, C. van Blitterswijk, B. Rousseau, O. Chassande, J. Amédée, J.-C. Fricain, Layer-by-layer tissue microfabrication supports cell proliferation in vitro and in vivo. Tissue Eng. Part C Methods **18**(1), 62–70 (2012)
60. H. Gudapati, J. Yan, Y. Huang, D.B. Chrisey, Biofabrication **6**(3), 035022 (2014)
61. Y. Deng, P. Renaud, Z. Guo, Z. Huang, Y. Chen, J. Biol. Eng. **11**, 1 (2017)
62. A. Prosperetti, A generalization of the Rayleigh-Plesset equation of bubble dynamics. Phys. Fluids **25**(3), 409–410 (1982)
63. L. Xiu-Mei et al., Growth and collapse of laser-induced bubbles in glycerolwater mixtures. Chin. Phys. B **17**(7), 2574–2579 (2008)
64. A. Pearson et al., Bubble interactions near a free surface. Eng. Anal. Bound Elem. **28**(4), 295–313 (2004)
65. P.B. Robinson et al., Interaction of cavitation bubbles with a free surface. J. Appl. Phys. **89**(12), 8225–8237 (2001)
66. C. Kryou, I. Theodorakos, P. Karakaidos, A. Klinakis, A. Hatziapostolou, I. Zergioti, Parametric Study of Jet/Droplet Formation Process during LIFT Bioprinting of Living Cell-Laden Bioink. Micromachines **12**, 1408 (2021)
67. M. Duocastella et al., Time-resolved imaging of the laser forward transfer of liquids. J Appl Phys **106**(8), 084907 (2009)
68. M. Ali, E. Pages, A. Ducom, A. Fontaine, F. Guillemot, Controlling laser-induced jet formation for bioprinting mesenchymal stem cells with high viability and high resolution. Biofabrication **6**, 045001 (2014)
69. M.S. Brown, N.T. Kattamis, C.B. Arnold, Time-resolved dynamics of laser-induced micro-jets from thin liquid films. Microfluid Nanofluid **11**(2), 199–207 (2011)
70. C. Mezel et al., Self-consistent modeling of jet formation process in the nanosecond laser pulse regime. Phys. Plasmas **16**(12), 12311212 (2009)
71. M.S. Brown, N.T. Kattamis, C.B. Arnold, Time-resolved study of polyimide absorption layers for blister-actuated laser-induced forward transfer. J. Appl. Phys. **107**(8), 083103 (2010)
72. W. Liu, Z. Zhong, N. Hu, Y. Zhou, L. Maggio, A.K. Miri, A. Fragasso, X. Jin, A. Khademhosseini, Y.S. Zhang, Coaxial extrusion bioprinting of 3D microfibrous constructs with cell-favorable gelatin methacryloyl microenvironments. Biofabrication **10**(2), 024102 (2018)
73. M. Gruene, C. Unger, L. Koch, A. Deiwick, B. Chichkov, Dispensing pico to nanolitre of a natural hydrogel by laser-assisted bioprinting. Biomed. Eng. **10**, 19 (2011)
74. R. Bradley et al., Laser bioprinting of pluripotent embryonal carcinoma cells. Tissue Eng **10**(3–4), 483–491 (2004)
75. W. Wei et al., Study of impact-induced mechanical effects in cell direct writing using smooth particle hydrodynamic method. J. Manuf. Sci. Eng. **130**(2), 021012–021110 (2008)
76. Z. Zhang, W. Chai, R. Xiong, L. Zhou, Y. Huang, Biofabrication **9**(2), 025038 (2017)
77. R. Xiong, Z. Zhang, W. Chai, Y. Huang, D.B. Chrisey, Biofabrication **1**, 1 (2015)
78. S.H. Mardikar, K. Niranjan, Observations on the shear damage to different animal cells in a concentric cylinder viscometer. Biotechnol. Bioeng. **68**(6), 697–704 (2000)
79. V. Keriquel, H. Oliveira, M. Remy, S. Ziane, S. Delmond, B. Rousseau, S. Rey, S. Catros, J. Amedee, F. Guillemot, J.C. Fricain, Sci. Rep. **7**(1), 1778 (2017)
80. P. Serra, M. Duocastella, J.M. Fernández-Pradas, J.L. Morenza, Appl. Surf. Sci. **255**(10), 5342–5345 (2009)
81. M. Gruene, A. Deiwick, L. Koch, S. Schlie, C. Unger, N. Hofmann, I. Bernemann, B. Glasmacher, B. Chichkov, Tissue Eng. Part C Methods **17**(1), 79–87 (2011)
82. J. M. Fernández-Pradas, Á. Rodríguez-Vázquez, M. Duocastella, M. Colina, G. Liñán-Cembrano, P. Serra, J. L. Morenza, Bioengineered and Bioinspired Systems III, Proc. SPIE Europe 2007
83. C.M. Othon, X. Wu, J.J. Anders, B.R. Ringeisen, Biomed. Mater. **3**(3), 034101 (2008)

84. C.Y. Chen, J.A. Barron, B.R. Ringeisen, Appl. Surf. Sci. **252**(24), 8641–8645 (2006)
85. R. Xiong, Z. Zhang, W. Chai, D.B. Chrisey, Y. Huang, Study of gelatin as an effective energy absorbing layer for laser bioprinting. Biofabrication **9**, 024103 (2017)
86. H. Desrus, B. Chassagne, S. Catros, C. Artiges , R. Devillarda, S. Petit, F. Deloison, J.C.. Fricain, F. Guillemot and R. Kling, Laser assisted bioprinting using a femtosecond laser with and without a gold transductive layer: a parametric study, Conference Paper · March 2016
87. S. Petit, O. Kérourédan, R. Devillard, E. Cormier, Femtosecond versus picosecond laser pulses for film-free laser bioprinting. Appl. Opt. **56**, 31 (2017)
88. S. Catros, J.-C. Fricain, B. Guillotin, B. Pippenger, R. Bareille, M. Remy, E. Lebraud, B. Desbat, J. Amédée, F. Guillemot, Laser-assisted bioprinting for creating on-demand patterns of human osteoprogenitor cells and nano-hydroxyapatite. Biofabrication **3**, 25001 (2011)
89. F. Guillemot, A. Souquet, S. Catros, B. Guillotin, J. Lopez, M. Faucon, B. Pippenger, R. Bareille, M. Rémy, S. Bellance, P. Chabassier, J.C. Fricain, J. Amédée, High-throughput laser bioprinting of cells and biomaterials for tissue engineering. Acta Biomater. **6**, 2494–2500 (2010)
90. A. Doraiswamy, R.J. Narayan, T. Lippert, L. Urech, A. Wokaun, M. Nagel, B. Hopp, M. Dinescu, R. Modi, R.C.Y. Auyeung, D.B. Chrisey, Excimer laser forward transfer of mammalian cells using a novel triazene absorbing layer. Appl. Surf. Sci. **252**, 4743–4747 (2006)
91. B. Hopp, T. Smausz, A. Nógrádi, in *Cell and Organ Bioprinting*. ed. by B.R. Ringeisen, B.J. Spargo, P.K. Wu (Springer, Dordrecht, 2010), pp.115–134
92. R. Xiong, Z. Zhang, W. Chai, D.B. Chrisey, Y. Huang, Biofabrication **9**(2), 024103 (2017)
93. E. Pagès, M. Rémy, V. Kériquel, M.M. Correa, B. Guillotin, F. Guillemot, J. Nanotechnol. Eng. Med. **6**(2), 021005 (2015)
94. V. Yusupov, S. Churbanov, E. Churbanova, K. Bardakova, A. Antoshin, S. Evlashin, P. Timashev, N. Minaev, Int. J. Bioprinting **6**(3), 271–271 (2020)
95. Biological laser bioprinting, a novel technique for creating heterogeneous 3-dimensional cell patterns. Biomed. Microdev. **6**, 139–214 (2004)
96. C.Y. Chen, J.A. Barron, B.R. Ringeisen, Cell patterning without chemical surface modification: cell-cell interactions between bovine aortic endothelial cells (BAEC) on a homogeneous cell-adherent hydrogel. Appl. Surf. Sci. **1**, 1 (2006)
97. J.A. Barron, B.J. Spargo, B.R. Ringeisen, Biological laser bioprinting of three dimensional cellular structures. App. Phys. A: Mater. Sci. Process. **79**, 1027–1030 (2004)
98. J.A. Barron, B.R. Ringeisen, H. Kim, B.J. Spargo, D.B. Chrisey, Application of laser bioprinting to mammalian cells. Thin Solid Films **453–454**, 383–387 (2004)
99. B.R. Ringeisen, H. Kim, J.A. Barron, D.B. Krizman, D.B. Chrisey, S. Jackman, R.Y.C. Auyeung, B.J. Spargo, Tissue Eng. **10**(3–4), 483–491 (2004)
100. L. Koch, S. Kuhn, H. Sorg, M. Gruene, S. Schlie, R. Gaebel, B. Polchow, K. Reimers, S. Stoelting, N. Ma, P.M. Vogt, G. Steinhoff, B. Chichkov, Tissue Eng. Part C Methods **16**(5), 847–854 (2010)
101. B. Hopp, T. Smausz, N. Kresz, N. Barna, Z. Bor, L. Kolozsvári, D.B. Chrisey, A. Szabó, A. Nógrádi, Tissue Eng. **11**(11–12), 1817–1823 (2005)
102. S. Catros, B. Guillotin, M. Bačáková, J.-C. Fricain, F. Guillemot, Appl. Surf. Sci. **257**(12), 5142–5147 (2011)
103. D. Riester, J. Laser Micro Nanoeng. **11**(2), 199–203 (2016)
104. J.A. Barron, P. Wu, H.D. Ladouceur, B.R. Ringeisen, Biological laser bioprinting: a novel technique for creating heterogeneous 3-dimensional cell patterns. Biomed. Microdev. **6**(2), 139–147 (2004)
105. B.R. Ringeisen, H. Kim, J.A. Barron, D.B. Krizman, D.B. Chrisey, S. Jackman et al., Laser bioprinting of pluripotent embryonal carcinoma cells. Tissue Eng. **10**(3–4), 483–491 (2004)
106. N.R. Schiele, D.T. Corr, Y. Huang, N.A. Raof, Y. Xie, D.B. Chrisey, Laser-based direct-write techniques for cell bioprinting. Biofabrication **2**(3), 32001 (2010)
107. Y. Lin, Y. Huang, G. Wang, T.-R.J. Tzeng, D.B. Chrisey, Effect of laser fluence on yeast cell viability in laser-assisted cell transfer. J. Appl. Phys. **106**(4), 043106 (2009)
108. J.A. Barron, D.B. Krizman, B.R. Ringeisen, Laser bioprinting of single cells: statistical analysis, cell viability, and stress. Ann. Biomed. Eng. **33**(2), 121–130 (2005)
109. C.Y. Chen, J.A. Barron, B.R. Ringeisen, Cell patterning without chemical surface modification: cell–cell interactions between printed bovine aortic endothelial cells (BAEC) on a homogeneous cell-adherent hydrogel. Appl. Surf. Sci. **252**(24), 8641–8645 (2006)
110. S. Catros, B. Guillotin, M. Bacáková, J.-C. Fricain, F. Guillemot, Effect of laser energy, substrate film thickness and bioink viscosity on viability of endothelial cells printed by Laser-Assisted Bioprinting. Appl. Surf. Sci. **257**(12), 5142–5147 (2011)
111. N.A. Raof, N.R. Schiele, Y. Xie, D.B. Chrisey, D.T. Corr, The maintenance of pluripotency following laser direct-write of mouse embryonic stem cells. Biomaterials **32**(7), 1802–1808 (2011)
112. M. Gruene, M. Pflaum, A. Deiwick, L. Koch, S. Schlie, C. Unger et al., Adipogenic differentiation of laser-printed 3D tissue grafts consisting of human adipose-derived stem cells. Biofabrication **3**(1), 15005 (2011)
113. A.J. Engler, S. Sen, H.L. Sweeney, D.E. Discher, Matrix elasticity directs stem cell lineage specification. Cell **126**, 677–689 (2006).
114. A.J. Engler, P.O. Humbert, B. Wehrle-Haller, V.M. Weaver, Multiscale modeling of form and function. Science **324**, 208–212 (2009)
115. P.K. Wu, B.R. Ringeisen, Development of human umbilical vein endothelial cell (HUVEC) and human umbilical vein smooth muscle cell (HUVSMC) branch/stem structures on hydrogel layers via biological laser bioprinting (BioLP). Biofabrication **2**, 014111 (2010)
116. S. Catros, B. Guillotin, M. Bacáková et al., Effect of laser energy, substrate film thickness and bioink viscosity on viability of endothelial cells printed by Laser-Assisted Bioprinting. Appl. Surf. Sci. **257**, 5142–5147 (2011)
117. L. Koch, S. Kuhn, H. Sorg et al., Laser bioprinting of skin cells and human stem cells. Tissue Eng. Part C Methods (2009). https://doi.org/10.1089/ten.tec.2009.0397
118. B. Guillotin, A. Souquet, S. Catros et al., Laser assisted bioprinting of engineered tissue with high cell density and microscale organization. Biomaterials **31**, 7250–7256 (2010)
119. M. Gruene, M. Pflaum, C. Hess et al., Laser bioprinting of three-dimensional multicellular arrays for studies of cell-cell and cell-environment interactions. Tissue Eng. Part C Methods **1**, 110629135038006 (2011)
120. N.R. Schiele, R.A. Koppes, D.T. Corr et al., Laser direct writing of combinatorial libraries of idealized cellular constructs: biomedical applications. Appl. Surf. Sci. **255**, 5444–5447 (2009)
121. N.A. Raof, N.R. Schiele, Y. Xie et al., The maintenance of pluripotency following laser direct-write of mouse embryonic stem cells. Biomaterials **32**, 1802–1808 (2011)
122. C.M. Othon, X. Wu, J.J. Anders, B.R. Ringeisen, Single-cell bioprinting to form threedimensional lines of olfactory ensheathing cells. Biomed Mater **3**, 034101 (2008)

123. D.B. Edelman, E.W. Keefer, A cultural renaissance: in vitro cell biology embraces threedimensional context. Exp. Neurol. **192**, 1–6 (2005)
124. D.E. Discher, D.J. Mooney, P.W. Zandstra, Growth factors, matrices, and forces combine and control stem cells. Science **324**, 1673 (2009)
125. T.G. Fernandes, M.M. Diogo, D.S. Clark, J.S. Dordick, J.M.S. Cabral, High-throughput cellular microarray platforms: applications in drug discovery, toxicology and stem cell research. Trends Biotechnol. **27**(6), 342 (2009)
126. V. Mironov, T. Boland, T. Trusk, G. Forgacs, R.R. Markwald, Organ bioprinting: computer-aided jet-based 3D tissue engineering. Trends Biotechnol. **21**(4), 157–161 (2003)
127. H.Y. Chang, Anatomic demarcation of cells: genes to patterns. Science **326**(5957), 1206–1207 (2009)
128. S.A. Ruiz, C.S. Chen, Emergence of patterned stem cell differentiation within multicellular structures. Stem Cells (Dayt Ohio) **26**(11), 2921–2927 (2008)
129. G. Vunjak-Novakovic, Patterning stem cell differentiation. Cell Stem Cell **3**(4), 362–363 (2008)
130. M. Gruene, M. Pflaum, C. Hess, S. Diamantouros, S. Schlie, A. Deiwick et al., Laser bioprinting of three-dimensional multicellular arrays for studies of cell-cell and cell-environment interactions. Tissue Eng. Part C Methods **17**, 973–982 (2011)
131. Y. Wu, L. Chen, P.G. Scott, E.E. Tredget, Mesenchymal stem cells enhance wound healing through differentiation and angiogenesis. Stem Cells **25**, 2648 (2007)
132. M. Hellström, M. Kalén, P. Lindahl, A. Abramsson, C. Betsholtz, Role of PDGF-B and PDGFR-β? In recruitment of vascular smooth muscle cells and pericytes during embryonic blood vessel formation in the mouse. Development **126**, 3047 (1999)
133. L. Koch, M. Gruene, C. Unger, B. Chichkov, Laser assisted cell bioprinting. Curr. Pharm. Biotechnol. **14**(1), 91–97 (2013)
134. L. Koch, A. Deiwick, S. Schlie, S. Michael, M. Gruene, V. Coger, D. Zychlinski, A. Schambach, K. Reimers, P.M. Vogt, B. Chichkov, Skin tissue generation by laser cell bioprinting. Biotechnol. Bioeng. **109**, 1855–1863 (2012)
135. R.L.H. Bigelow, E.Y. Jen, M. Delehedde, N.S. Chari, T.J. McDonnell, Sonic hedgehog induces epidermal growth factor dependent matrix infiltration in HaCaT keratinocytes. J. Investig. Dermatol. **124**, 457 (2005)
136. C. Linge, Establishment and maintenance of normal human keratinocyte cultures, in *Methods in Molecular Medicine, 2nd edition, Human Cell Culture Protocols*, vol. 107, ed. by J. Picot (Humana Press Inc., Totowa, 2004), p.1
137. C.M. Niessen, Tight junctions/adherens junctions: basic structure and function. J. Investig. Dermatol. **127**, 2525–2532 (2007)
138. G. Mese, G. Richard, T.W. White, Gap junctions: basic structure and function. J. Investig. Dermatol. **127**, 2516–2524 (2007)
139. S. Michael, H. Sorg, C.-T. Peck, L. Koch, A. Deiwick, B. Chichkov, P.M. Vogt, K. Reimers, Tissue engineered skin substitutes created by laser-assisted bioprintingform skin-like structures in the dorsal skin fold chamber inmice. PLoS ONE **8**(3), 57741 (2013)
140. Y. Nahmias, R.E. Schwartz, C.M. Verfaillie, D.J. Odde, Laser-guided direct writing for three-dimensional tissue engineering. Biotechnol. Bioeng. **92**(2), 129–136 (2005)
141. P.K. Wu, B.R. Ringeisen, Development of human umbilical vein endothelial cell (HUVEC) and human umbilical vein smooth muscle cell (HUVSMC) branch/stem structures on hydrogel layers via biological laser bioprinting (BioLP). Biofabrication **2**(1), 14111 (2010)
142. R.K. Pirlo, P. Wu, J. Liu, B. Ringeisen, PLGA/hydrogel biopapers as a stackable substrate for bioprinting HUVEC networks via BioLP. Biotechnol. Bioeng. **109**(1), 262–273 (2012)
143. P.C.H. Hsieh, M.E. Davis, L.K. Lisowski, R.T. Lee, Endothelial-cardiomyocyte interactions in cardiac development and repair. Annu. Rev. Physiol. **68**, 51–66 (2006)
144. T.M. Patz, A. Doraiswamy, R.J. Narayan, W. He, Y. Zhong, R. Bellamkonda et al., Three-dimensional direct writing of B35 neuronal cells. J. Biomed. Mater. Res. B **78**(1), 124–130 (2006)
145. A. Ramón-Cueto, F. Valverde, Olfactory bulb ensheathing glia: a unique cell type with axonal growth-promoting properties. Glia **14**(3), 163–173 (1995)
146. C.M. Othon, X. Wu, J.J. Anders, B.R. Ringeisen, Single-cell bioprinting to form three-dimensional lines of olfactory ensheathing cells. Biomed. Mater. **3**(3), 34101 (2008)
147. N.R. Schiele, R.A. Koppes, D.T. Corr, K.S. Ellison, D.M. Thompson, L.A. Ligon et al., Laser direct writing of combinatorial libraries of idealized cellular constructs: biomedical applications. Appl. Surf. Sci. **255**(10), 5444–5447 (2009)
148. J.L. Curley, S.C. Sklare, D.A. Bowser, J. Saksena, M.J. Moore, D.B. Chrisey, Isolated node engineering of neuronal systems using laser direct write. Biofabrication **8**(1), 15013 (2016)
149. R. Gaebel, N. Ma, J. Liu, J. Guan, L. Koch, C. Klopsch et al., Patterning human stem cells and endothelial cells with laser bioprinting for cardiac regeneration. Biomaterials **32**(35), 9218–9230 (2011)
150. Z. Ma, Q. Liu, H. Yang, R.B. Runyan, C.A. Eisenberg, M. Xu et al., Laser patterning for the study of MSC cardiogenic differentiation at the single-cell level. Light Sci. Appl. **2**(5), 68 (2013)
151. C.J.P. Colón, I.L. Molina-Vicenty, M. Frontera-Rodríguez, A. García-Ferré, B.P. Rivera, G. Cintrón-Vélez, S. Frontera-Rodríguez, Muscle and bone mass loss in the elderly population: advances in diagnosis and treatment. J. Biomed (Syd). **3**, 40–49 (2018)
152. M.I. Santos, R.L. Reis, Vascularization in bone tissue engineering: physiology, current strategies, major hurdles and future challenges. Macromol. Biosci. **10**(1), 12–27 (2009)
153. W. Wang, K.W.K. Yeung, Bone grafts and biomaterials substitutes for bone defect repair: a review. Bioact. Mater. **2**(4), 224–247 (2017)
154. B. Birru, N. Kumar Mekala, S. Rao Parcha, Mechanistic role of perfusion culture on bone regeneration. J. Biosci. **44**, 23 (2019)
155. H. Petite, V. Viateau, W. Bensaïd, A. Meunier, C. de Pollak, M. Bourguignon et al., Tissue-engineered bone regeneration. Nat. Biotechnol. **18**(9), 959–963 (2000)
156. A. Doraiswamy, R.J. Narayan, M.L. Harris, S.B. Qadri, R. Modi, D.B. Chrisey, Laser microfabrication of hydroxyapatite-osteoblast-like cell composites. J. Biomed. Mater. Res. A **80A**(3), 635–643 (2007)
157. S. Catros, J.-C. Fricain, B. Guillotin, B. Pippenger, R. Bareille, M. Remy et al., Laser-assisted bioprinting for creating on-demand patterns of human osteoprogenitor cells and nano-hydroxyapatite. Biofabrication **3**(2), 25001 (2011)
158. V. Keriquel, F. Guillemot, I. Arnault, B. Guillotin, S. Miraux, J. Amédée et al., In vivo bioprinting for computer- and robotic-assisted medical intervention: preliminary study in mice. Biofabrication **2**(1), 14101 (2010)